CHARACTERIZATION OF THE CHEMICAL BEHAVIOR OF A DBD WIRE-CYLINDER REACTOR FOR NO_X REMOVAL. DETERMINATION OF REACTIONAL PATHWAYS BY ISOTOPIC LABELING

A. VINCENT, F. DAOU, and J. AMOUROUX

Laboratoire de **G**énie des **P**rocédés **P**lasmas et **T**raitements de **S**urfaces
Université Pierre et Marie CURIE (Paris VI)
ENSCP – 11, rue Pierre et Marie CURIE
75231 PARIS cedex 05 - France

ABSTRACT:

The aim of this work is to determine the chemical reactivity of the DBD wire-cylinder reactor in order to control the NO_x removal in a mixture of gases representing exhaust engine gases. Therefore we will qualify and quantify the major by-products of the treatment of an O_2 (10%), CO_2 (10%), H_2O (5.4%), C_3H_6 (1000ppmv), NO (1000ppmv) and N_2 (balance) mixture at atmospheric pressure and 100°C. We can observe the presence of VOC's like aldehyde (especially formaldehyde, acetaldehyde and propanal) and of R-NOx (particularly CH_3-O-NO_2, nitromethane and C_2H_5-O-NO_2). We can also notice the increase of these by-products with the increase of the energy density. Finally, we demonstrate that the creation of R-NO_x is due to the oxidation of C_3H_6 fragments by O_2 and not by CO_2 contrary to acetaldehyde and propanal.

Keywords: DBD, NO_x removal, Wire-cylinder, GC-MS, reactional mechanisms, isotopic labeling

1. INTRODUCTION

NO_x emissions are a major preoccupation in pollution control. It imposes new processes developments. Corona discharge treatment can efficiently be applied to polluted gases in order to reduce the undesirable emissions[1,2,3]. Many applications of DC and AC corona discharge for NO_x conversion are well known, using point-to-plane[3,4,5], multipoint-to-plane[4,6,7] or wire-cylinder [8,9] reactors. This removal of NO_x by dielectric barrier discharge treatment can be occurred by oxidation of NO in NO_2 and formation of nitric acid by reaction with water, reduction or trapping by hydrocarbons. That's the reason we analyze by-products contained in treated gas by GC-MS, allowing the identification and the quantification of produced carbon compounds. This analyze needs a previous electrical qualification based on voltage, current, charge and power measurements with a digital oscilloscope.

The analyze of a plasma treated O_2 (10%), CO_2 (10%), H_2O (5.4%), C_3H_6 (1000ppmv), NO (1000ppmv) and N_2 (balance) gas mixture is presented in this paper. The reactor is a wire-cylinder dielectric barrier discharge one and is connected to an AC high voltage generator.

The main by-products will be quantified depending on energy density injected in the plasma. After it, we will determine the reactional pathways by substituting introduced O_2 by its $^{18}O_2$ isotope. The mass spectrum of the different species created by oxidation from O_2 will indeed be modified. Then we will be able to understand the chemical behavior of the DBD reactor.

2. EXPERIMENTAL SET-UP

As shown in Fig. 1 and Fig. 2, the reactor is a cylindrical dielectric pipe (aluminio-silicate pipe: $Ø_{int}$=15mm / $Ø_{ext}$=21mm + glass pipe within aluminio-silicate pipe: $Ø_{int}$=11mm / $Ø_{ext}$=15mm). The high voltage electrode is a 6mm diameter copper screw (gap=2.5mm) and the grounded electrode is a sheet of copper. Energy is supplied by a “Calvatron SG2” high voltage 44kHz AC supply (applied voltage is between 12 and 16kV peak to peak). Electrical characterization is made measuring voltage (using a high voltage 1:1000 probe), current, power, electric charge, frequency and pulse time by a 500MHz digital oscilloscope (LeCroy LT 342). The reactor is fed with a gas mixture at atmospheric pressure. Each gas (except water vapor) is introduced in the reactor by a mass flow meter. O_2 (10%), CO_2 (10%) and N_2 (balance) are introduced in a heating cartridge while NO (1000ppmv) and C_3H_6 (1000ppmv) are introduced after it. We also avoid NO and C_3H_6 transformation on the inner walls of the cartridge. A motorized syringe pusher introduces H_2O (5.4%) in a heated 1/8” diameter and 2 meters long stainless steel pipe. Vaporized water is then introduced in heated gas. The total gas flow is about 12.9 slpm (slpm means $L.min^{-1}$ in normalized conditions: atmospheric pressure and 0°C) or 17.4$L.min^{-1}$ at 100°C (experimental temperature). Gas mixture temperature is measured by a thermocouple at 3 centimeters after the discharge zone.

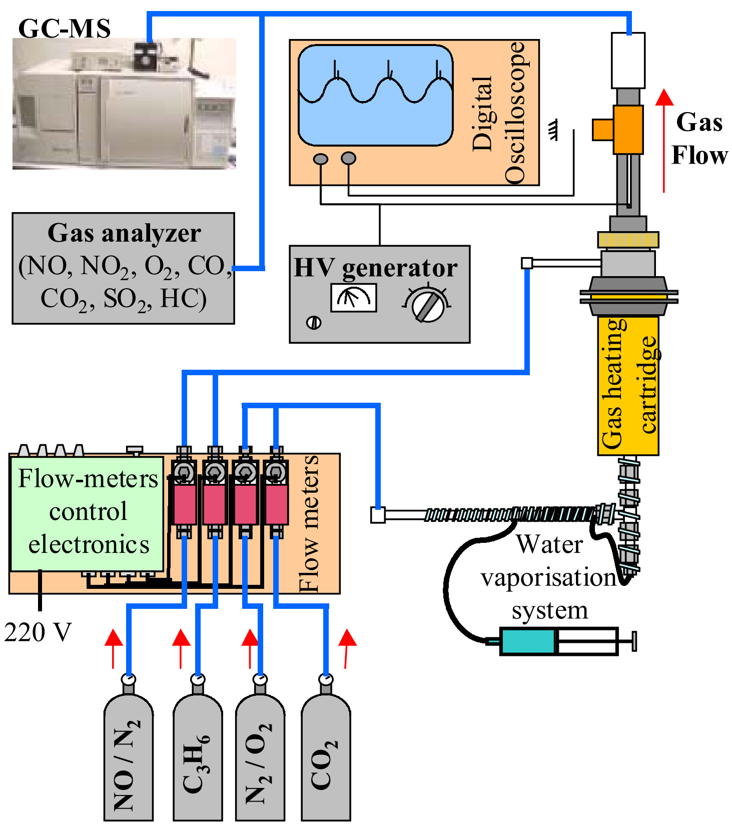

Fig. 1. Experimental set-up of the wire-cylinder reactor, gas feeding system and analysis apparatus

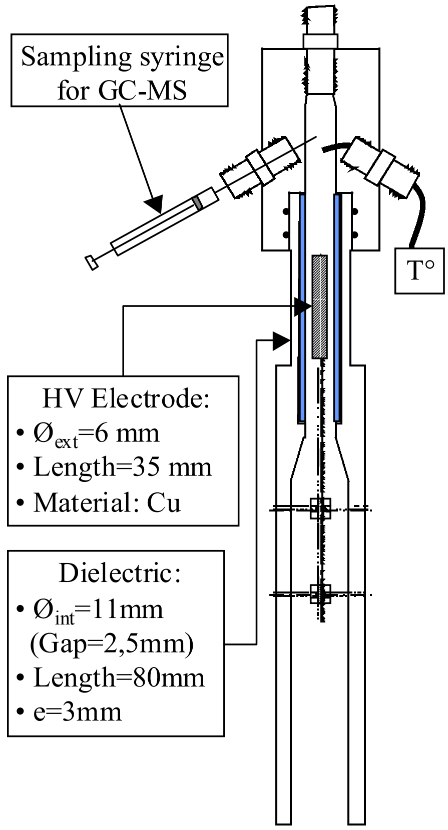

Fig. 2. Detailed schema of the wire-cylinder reactor

Gas analysis apparatus:

The treated gas flows from the reactor to the different analysis apparatus through a heated 1/4” stainless steel pipe. The in-line analyzers are:

- GC-MS (Gas Chromatography coupled with a Mass Spectrometer): it allows the identification (sensitivity: 1 to 10 ppm depending on the compound) and the quantification (± 5% after calibration) of the different hydrocarbons to provide the carbon mass balance. The chromatographic column is a Chrompack PoraPlotQ (25m-0.32mm-10µm, divinyl-benzen polystyren). Gas introduction is made with a 100µl 6 ways gas sampler, carrier gas is He (pressure: 0.3 kg.cm^{-2}).
- QUINTOX Gas Analyzer (measuring NO, NO_2, O_2, CO_2, CO, SO_2 quantities): performances are indicated in the Table I.

Gas measurement	Range	Accuracy	Resolution
O_2	0-25 %	0.1 à 0.2 %	0.1 %
CO	0-10000 ppm	20 ppm : [CO] < 400 ppm 5 % : [CO] < 2000 ppm 10 % : [CO] > 2000 ppm	1 ppm
	0.1-10 %	+/- 5 %	0.01 %
NO	0-5000 ppm	5 ppm : [NO] < 100 ppm 5 % : [NO] > 100 ppm	1 ppm
NO_2	0-1000 ppm	+/- 5 ppm	1 ppm
SO_2	0-5000 ppm	5 %	1 ppm
CO_2	0-fuel value	+/- 0.3 %	0.1 %
Hydrocarbons (HC)	0-5 % Méthane	5 %	0.01 %

Table I: *Utilization range, accuracy and resolution of the gas analyzer*

- DRÄGER Colorimetric detector tubes (measuring NO + NO_2 or CO quantity): the utilization range and precision are:

  NO + NO_2 : 50 – 2500 ppm ± 10%

  CO : 25 – 1000 ppm ± 5%

NO_x analysis with gas analyzer and colorimetric detector were validated after measurements of NO_x at the exit of a NO/N_2 gas bottle (NO: 1800ppmv) and after a 1:1 dilution with N_2 using the mass flow-meters.

3. EXPERIMENTAL RESULTS – DISCUSSION

3.1. Electrical characterization of the reactor:

Electrical characterization of a reactor[9,10] is the prerequisite to the chemical study. It is an important step in energy balance determination and control of energy consumption[11]. Measuring voltage, current, frequency and charge has provided the electrical behavior of the reactor. A previous study[9] has been carried with various physical parameters (change of the material of electrode and dielectric, the gap, the gas flow or heating and hydration).

For this work, where only hydration is a variable parameter, the electrical measurements are summed up in the Fig. 3 and Table II.

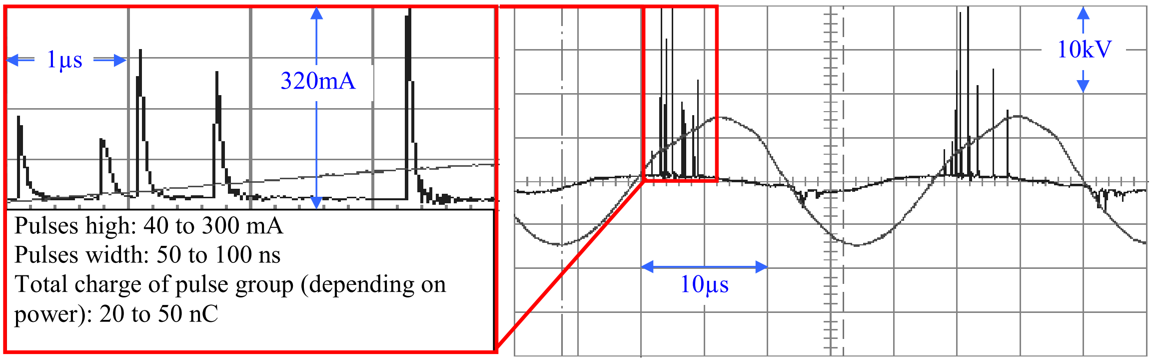

Fig. 3. *Oscillogram obtained for the treatment of the O_2 (10%), CO_2 (10%), H_2O (5.4%), C_3H_6 (1000ppmv), NO (1000ppmv) and N_2 (balance) gas mixture (U_{pkpk}=14.5kV, frequency=44kHz, T=180°C, flow=12.9 slpm)*

Table II. *Different electrical measures obtained for the treatment of the O_2 (10%), CO_2 (10%), H_2O (0 or 5.4%), C_3H_6 (1000ppmv), NO (1000ppmv) and N_2 (balance) gas mixture (T=100 to 180°C depending on discharge power, flow=12.9 slpm) at various voltages*

	0% water			5.4% water			
Voltage (kV_{pkpk})	13.0	13.5	14.3	12.8	13.3	13.6	14.4
Frequency (kHz)	44.0			44.0			
Intensity (mA)	3.9	5.5	3.9	2.9	3.7	5.7	8.0
Power (W)	18	26	42	13	18	27	41
Energy density (J/L)	54	79	126	39	53	82	122
Charge of the pulses group (nC)	27	38	51	20	30	41	
Elementary charges / second (10^{-6}mol.s^{-1})	0.45	0.62	0.84	0.32	0.50	0.67	

The usable voltage range is here 12.8 to 14.4kV_{pkpk}. It allows the achievement of a corona discharge mode with stable multiple impulsions adapted to NO_x removal. The current versus energy density diagram has been both determined under wet and dry conditions (Fig. 4). The temperature conditions were not constant for the different measures because the gas is heated by the discharge proportionally to its power.

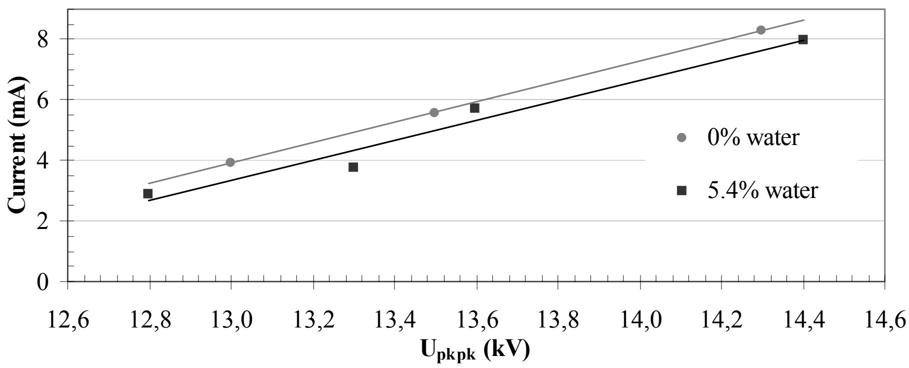

Fig. 4. *Current vs. voltage curve obtained for the treatment of the O_2 (10%), CO_2 (10%), H_2O (0 or 5.4%), C_3H_6 (1000ppmv), NO (1000ppmv) and N_2 (balance) gas mixture (T=100 to 180°C depending on discharge power, flow=12.9 slpm)*

We can observe that hydration has a weak influence on the current vs. voltage characterization. Nevertheless, hydration decreases a bit the breakdown voltage. We should notice that current measured is an average current: the current of the pulses represents only a part of it. The interesting part of current is the pulse's one which is due to the electron crossing the gap and creating excited, ionized and dissociated species. Those species are responsible of the chemical activity of the plasma through the reaction with neutral molecules and create a great variety of hydrocarbon compounds and R-NO_x.

3.2. Characterization of the depollution treatment: analysis of the treated gas

Analyses were conducted at different applied power to qualify the depollution behavior of the reactor versus energy density. Before each analysis (simultaneously made by GC-MS and gas analyzer), a measure was made with the discharge off. Two series of analyses were conducted: one without water vapor in the gas mixture, another with 5.4% of water vapor.

- NO_x measurements with gas analyzer:

The measures of NO and NO_2 concentrations after the treatment of the gas mixture without water vapor and with 5.4% of water vapor are presented in Fig. 5.

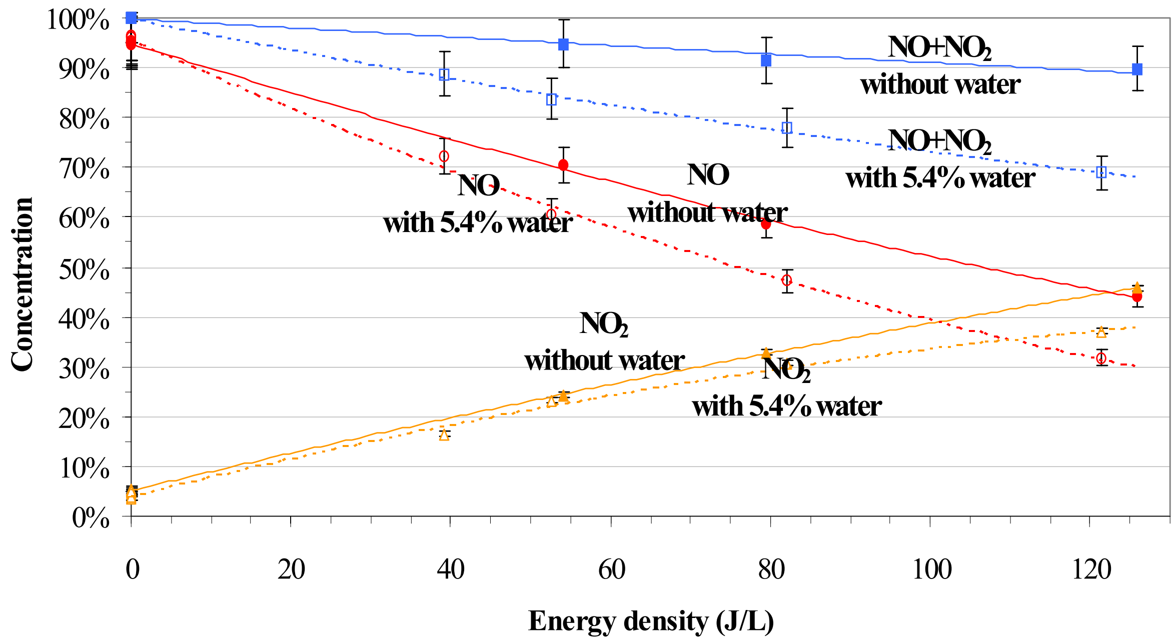

Fig. 5. *NO_x concentration vs. energy density of the dry or hydrated O_2 (10%), CO_2 (10%), H_2O (0 or 5.4%), C_3H_6 (1000ppmv), NO (1000ppmv) and N_2 (balance) gas mixture (T=100 to 180°C depending on discharge power, flow=12.9 slpm)*

First, we can notice that NO concentration decreases with energy density increase. This decrease of NO is linked to the NO_2 increase through oxidation processes. The oxidant vector can be O_2 (giving O in the discharge)[12], CO_2 (giving O and CO)[13,14] and H_2O (giving OH)[15,16,17]. Those species are present in excess in the mixture (about 100 to 1 NO molecule). But a significant part of NO "disappears", being trapped by C_3H_6 and its fragments giving R-NO_x[18], adsorbed on the outlet pipes or reduced to N_2+O_2. R-NO_x formation will be presented in the following section.

Another important information of those analyses is the role of water in the mixture. It strongly increases the NO_x removal (30% vs. 10%). This can be partially due to the formation of HNO_3 by reaction with water vapor through OH formation but we can also connect this result to the decrease of voltage and power necessary to the gas treatment: the water makes the discharge easier to obtain.

- VOC and R-NO_x measurements with GC-MS

GC-MS was used to determine the different carbon by-products (under C_4) contained in the gas phase after plasma treatment. Two families of compounds, all issued from C_3H_6 fragmentation in the discharge has been identified: VOC and R-NO_x. VOC are essentially composed of aldehydes (formaldehyde, acetaldehyde, propanal…) but there are also weak quantities of propenal, acetone, methanol and ethanol (Fig. 6).

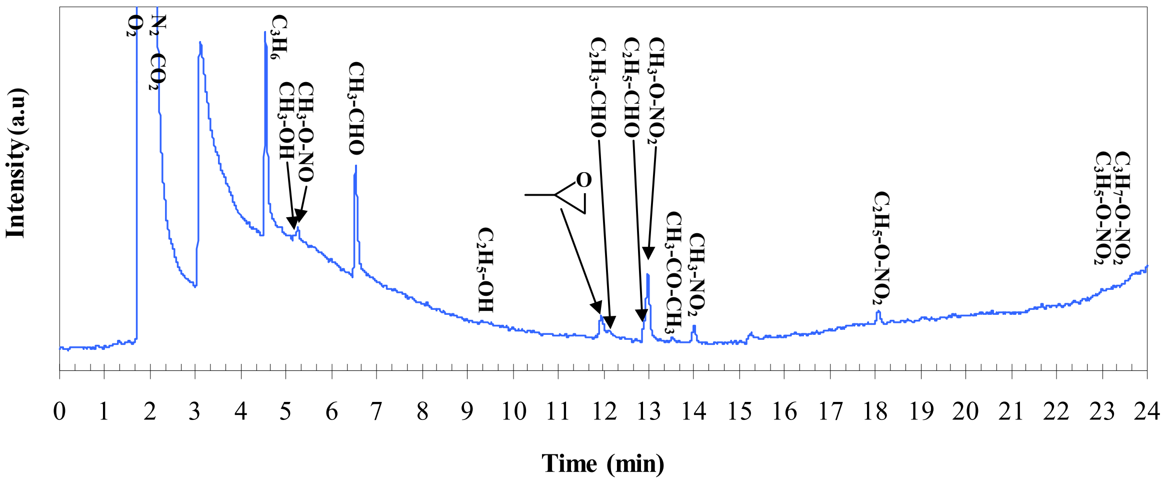

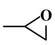 represents the propylene oxide and will be noted CH_3-$HCOCH_2$.

Fig. 6. *Chromatogram of a plasma treated O_2 (10%), CO_2 (10%), H_2O (5.4%), C_3H_6 (1000ppmv), NO (1000ppmv) and N_2 (balance) gas mixture (T=140°C, flow=12.9 slpm)*

The majority of R-NO_x observed is based on a CH_3 function (CH_3-O-NO, CH_3-O-NO_2 and CH_3-NO_2) but there are also some quantities of C_2 and C_3 R-NO_x (C_2H_5-O-NO_2, C_3H_5-O-NO_2 and C_3H_7-O-NO_2). Absolute quantities of C_3H_6 (introduced or remaining after the plasma treatment) have been determined. Most of the other by-products are not stable enough (excepted nitromethane) to be proposed in fine chemicals dealer catalogs, so only relative quantification has been carried (comparison of the peak areas between two chromatograms at different energy density).

Fig. 7.1 and Fig. 7.2 indicates the relative concentration vs. energy density of the different analyzed species.

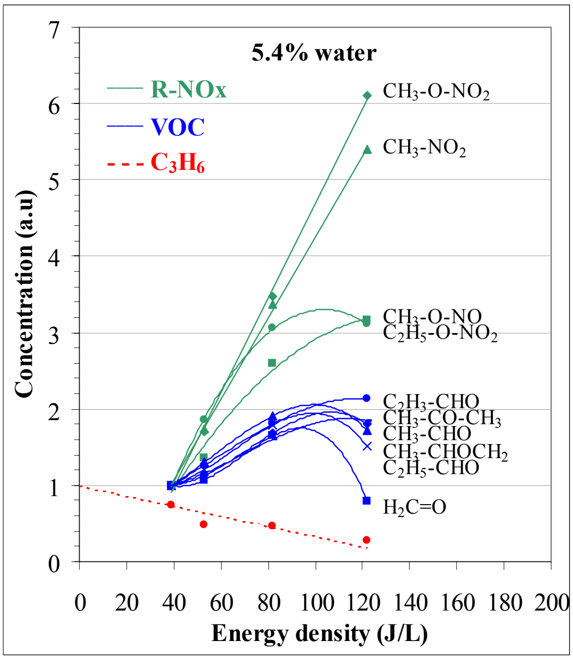

Fig. 7.1. Quantitative variation of C_3H_6 and by-products depending on energy density for an O_2 (10%), CO_2 (10%), H_2O (5.4%), C_3H_6 (1000ppmv), NO (1000ppmv) and N_2 (balance) gas mixture (T=100 to 180°C depending on discharge power, flow=12.9 slpm)

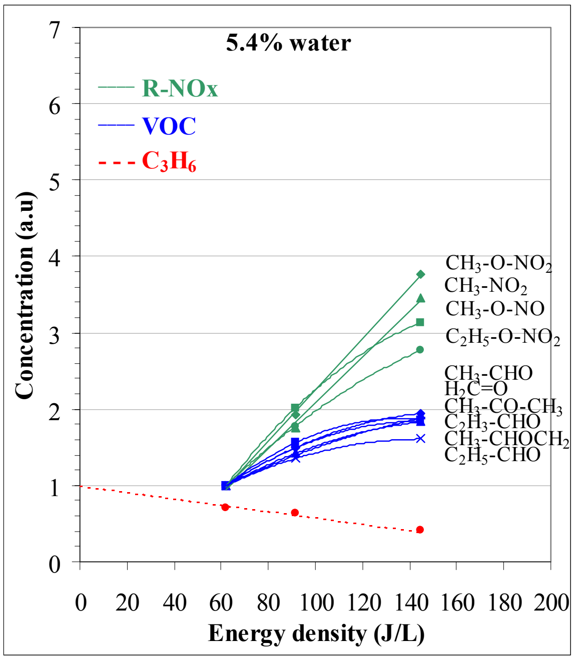

Fig. 7.2. Quantitative variation of C_3H_6 and by-products depending on energy density for an O_2 (10%), CO_2 (10%), C_3H_6 (1000ppmv), NO (1000ppmv) and N_2 (balance) dry gas mixture (T=100 to 180°C depending on discharge power, flow=12.9 slpm)

In each case, the first value of concentration is arbitrary set to 1. The other concentrations are also calculated relatively to this first measure. In the case C_3H_6, it has been obtained at 0 $J.L^{-1}$ because propylene is introduced in the mixture before the treatment. For the other compounds, the initial value has been carried at the minimal energy to trigger the discharge.

We can notice that R-NO_x quantity greatly increases with energy density while VOC quantity increases and stagnate with energy density. There are also two typical behaviors depending on chemical family: R-NO_x or VOC. Those behaviors are quite the same with or without water vapor except for the energy density scale. If we contract the scale of Fig. 7.2 from 145 to 85 $J.L^{-1}$, both figures can be overlapped. The presence of water vapor seems to reduce the energy density needed to treat as well the gas mixture. In other words, at constant energy density, the treatment is more efficient with water vapor.

3.3. Determination of reactional mechanism by isotopic labeling

Once we have determinated the reactivity in the reactor vs. energy density, we are interested in understanding the reactional mechanism occurring in the by-products creation. First we can propose different mechanism using the introduced species and the supposed radicals or fragments produced in the discharge. Then, we have substituted one of the introduced species by its isotope and we determine with GC-MS the changes in by-products. We also can determine the reactional pathway.

In our case, we could see that by-products are all created by oxidation of C_3H_6 or its fragments. Then we substituted O_2 (^{16}O-^{16}O) by labeled O_2 (^{18}O-^{18}O). We also can determinate if O in molecules comes from O_2 (^{18}O labeled by-product), from CO_2 (unlabeled by-product) or from the both (partially ^{18}O labeled by-product). For example, we'll take the case of acetone. It can be produced by the attack of C_3H_6 by O_2 (100% labeled CH_3-CO-CH_3). It can also be produced by the attack of C_3H_6 by O giving partially labeled acetone. O atoms comes indeed from O_2 and CO_2 fragmentation in the discharge: O_2 producing ^{18}O while CO_2 produces ^{16}O, both ^{16}O and ^{18}O atoms are present in the mixture. Finally, acetone can be produced by binding of CO with two CH_3 radicals (coming from C_3H_6 fragmentation) giving a totally unlabeled molecule.

The determination of the reactional mechanisms requires the knowledge of the by-products mass spectrum and its possible changes in labeling. For example, in the CH_3-O-NO_2 mass spectrum, the m/z=15, 29, 46 & 76 peaks are representatives of CH_3, CH-O, NO_2, and CH_3-NO_3 fragments. In the case of an $^{18}O_2$ labeled molecule, m/z=15 will be unchanged while m/z=29, 46, 76 can be changed in m/z=31; 48 or 50; 78, 80 or 82 for CH-$\mathbf{^{18}O}$, N^{16}O$\mathbf{^{18}O}$ or N$\mathbf{^{18}O^{18}O}$, and CH_3-N^{16}O^{16}O$\mathbf{^{18}O}$, CH_3-N^{16}O$\mathbf{^{18}O^{18}O}$ or CH_3-N$\mathbf{^{18}O^{18}O^{18}O}$ fragments. The ratio between the different peak areas gives the proportion of each isotope produced by the discharge. Fig. 8.1 to Fig. 8.4 presents the different peaks for these particular m/z.

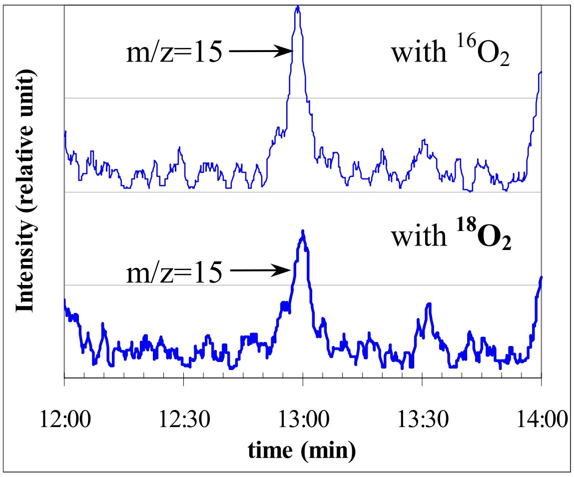

Fig. 8.1. *Chromatogram of CH_3-O-NO_2 for CH_3 fragment (m/z = 15)*

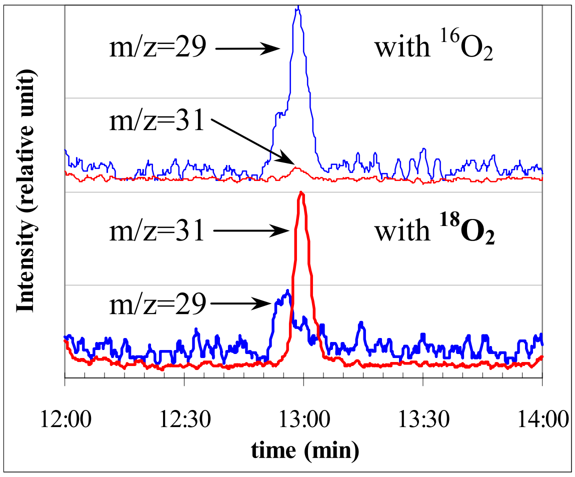

Fig. 8.2. *Chromatogram of CH_3-O-NO_2 for CH-O fragment (m/z = 29 and 31)*

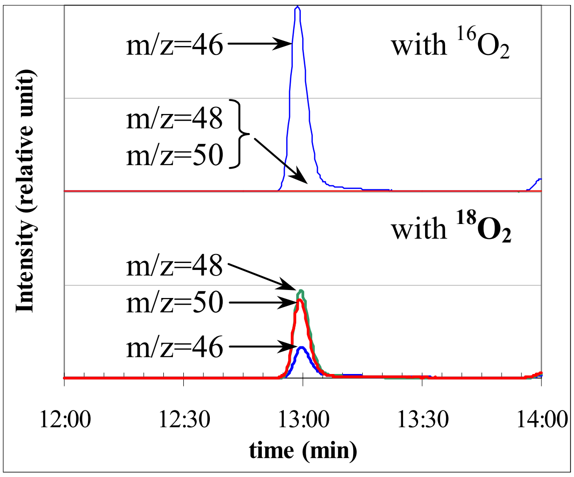

Fig. 8.3. *Chromatogram of CH_3-O-NO_2 for NO_2 fragment (m/z = 46, 48 and 50)*

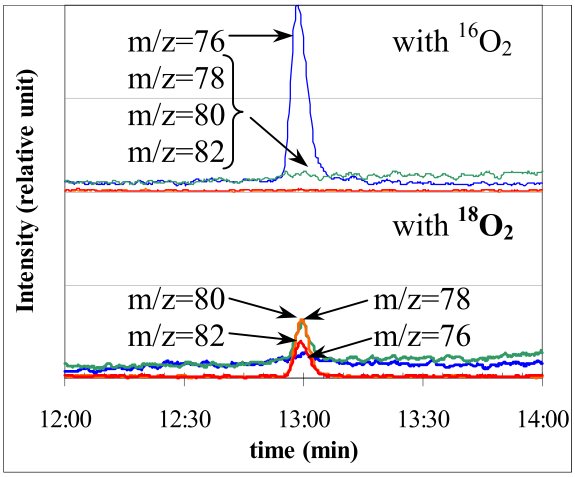

Fig. 8.4. *Chromatogram of CH_3-O-NO_2 native peak (m/z = 76, 78, 80 and 82)*

The analysis of Fig. 8.2 indicates that ^{18}O labeled mixture totally changes the m/z=29 into m/z=31 peak (the remaining m/z=29 peak on the lower curve is due to the 12'55" propanal peak while CH_3-O-NO_2 peak is centered on 13'00"). Then the O atom between CH_3 and NO_2 functions is due to the oxidation of CH_3 radicals by $^{18}O_2$ initially introduced. The Fig. 8.3 indicates that NO_2 function contains about 10% of $N^{16}O^{16}O$, 50% of $N^{16}O^{\mathbf{18}}\mathbf{O}$ and 40% of $N^{\mathbf{18}}\mathbf{O}^{\mathbf{18}}\mathbf{O}$ (calculated by the peak area ratio balanced with noise level). Those values are corroborated by Fig. 8.4 that indicates the absence of m/z=76 peak, the small m/z=78 peak and quasi-equivalence of m/z=80 and m/z=82 peaks. We can notice that a great part of NO_2 trapped in this molecule doesn't come from the native NO (which is unlabeled) but was produced from N_2 and $^{18}O_2$ by the discharge. The other part is essentially due to oxidation of native NO by ^{18}O and caught by CH_3-^{18}O (created from CH_3 and $^{18}O_2$). CH_3-$^{\mathbf{18}}\mathbf{O}$-$N^{16}O^{16}O$ should have been created by oxidation of NO with ^{16}O coming from CO_2.

Proceeding with the same methodology allows us to determine the isotopic composition of the different by-products. These compositions are summed up in the Table III.

Specie	**Fragment or molecule isotope**	**Proportion**	**Source of O**
CH_3-CHO	CH_3-$CH^{16}O$	**95%**	CO (from CO_2)
	CH_3-$CH\mathbf{^{18}O}$ *	5%	
CH_3-$HCOCH_2$	CH_3-$CH^{16}OCH_2$	15%	O (from O_2)
	CH_3-$CH\mathbf{^{18}O}CH_2$ *	**85%**	
C_2H_3-CHO	C_2H_3-$CH^{16}O$	25%	O (from O_2)
	C_2H_3-$CH\mathbf{^{18}O}$ *	**75%**	
C_2H_5-CHO	C_2H_5-$CH^{16}O$	**80%**	CO (from CO_2)
	C_2H_5-$CH\mathbf{^{18}O}$ *	20%	
CH_3-CO-CH_3	CH_3-$C^{16}O$-CH_3	**40%**	O (from O_2 & CO_2)
	CH_3-$C\mathbf{^{18}O}$-CH_3 *	**60%**	
CH_3-O-NO	CH_3-^{16}O-$N^{16}O$	13%	O (from O_2) & NO
	CH_3-$\mathbf{^{18}O}$-$N^{16}O$ *	**60%**	
	CH_3-$\mathbf{^{18}O}$-$N\mathbf{^{18}O}$ *	27%	
CH_3-O-NO_2	CH_3-$\mathbf{^{18}O}$-$N^{16}O^{16}O$ *	10%	O (from O_2) & NO
	CH_3-$\mathbf{^{18}O}$-$N^{16}O\mathbf{^{18}O}$ *	50%	
	CH_3-$\mathbf{^{18}O}$-$N\mathbf{^{18}O^{18}O}$ *	40%	
CH_3-NO_2	CH_3-$N^{16}O^{16}O$	20%	O (from O_2) & NO
	CH_3-$N^{16}O\mathbf{^{18}O}$ *	55%	
	CH_3-$N\mathbf{^{18}O^{18}O}$ *	25%	
C_2H_5-O-NO_2 C_3H_5-O-NO_2 C_3H_7-O-NO_2	$N^{16}O^{16}O$	15%	O (from O_2) & NO
	$N^{16}O\mathbf{^{18}O}$ *	80%	
	$\mathbf{N^{18}O^{18}O}$ *	5%	

* signals an ^{18}O containing molecule

Table III. *Composition of the by-products obtained for the treatment of an $^{18}O_2$ (10%), CO_2 (10%), H_2O (5.4%), C_3H_6 (1000ppmv), NO (1000ppmv) and N_2 (balance) gas mixture (T=140°C, flow=12.9 slpm)*

In this table, we couldn't indicate the isotopic composition of formaldehyde and alcohol's because the peaks are too weak or too noisy to be interpreted. We didn't present the CO_2 labeling too because its m/z=44 peak was saturated but we could measure an increase of the m/z=48 peak ($C^{18}O^{18}O$) in a rate of 1:40, illustrating the exchange of O atoms between CO_2 and O_2.

The main R-NOx emitted (CH_3-O-NO, CH_3-O-NO_2 and CH_3-NO_2) are essentially produced by oxidation of NO by O (itself essentially due to O_2) but it contains a significant part of NO_2 created from N_2 & O_2 in the discharge. For the main VOC emitted (acetaldehyde, propanal and propylene oxide) the two first are essentially produced by oxidation of HC fragments with CO while CH_3-$HCOCH_2$ is directly formed by oxidation of C_3H_6 with O (from O_2 and CO_2). The Fig. 9 gives a summary of the main results concerning the origin of the different by-products:

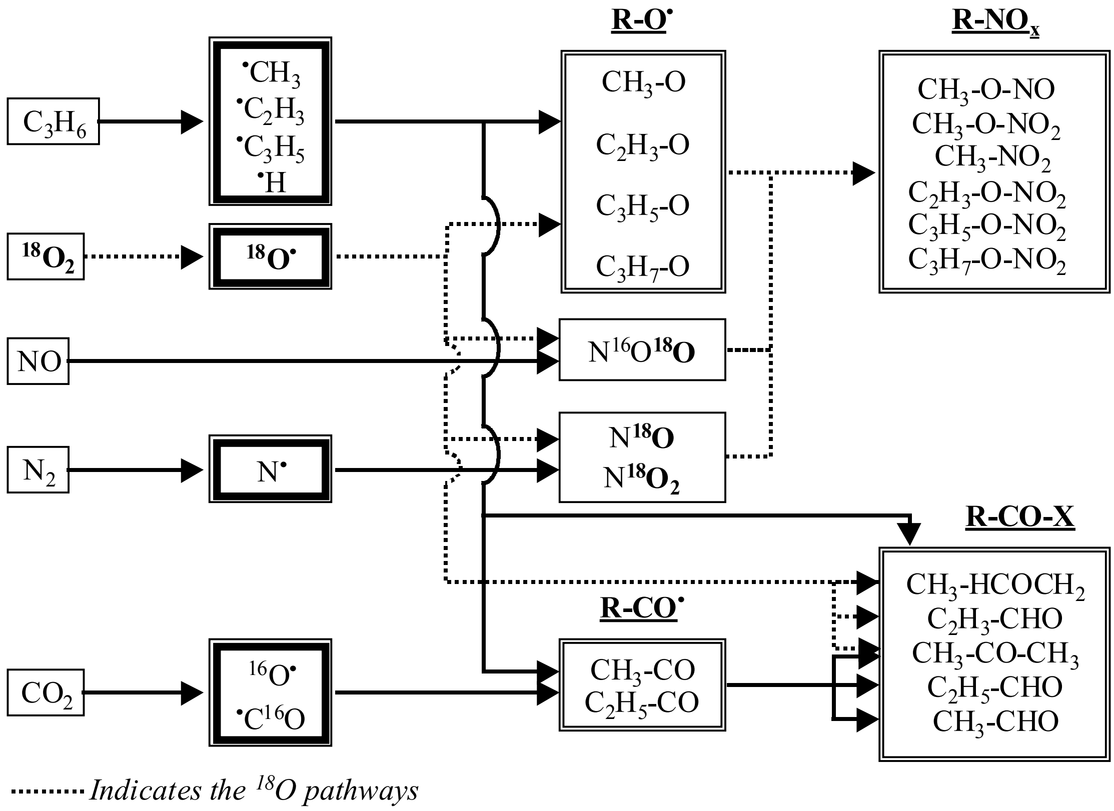

Fig. 9. *Determination by isotopic labeling ($O_2 \rightarrow {}^{18}O_2$) of reactional pathways conducting to the formation of the VOC's and R-NO_x*

4. CONCLUSION

This study was performed with two goals: qualify and quantify the behavior of the wire-cylinder as a chemical reactor by measuring the by-products formation versus energy density and determining the reactional pathways conducting to it. The understanding of this chemistry requires knowing the electrical behavior of the reactor. Then, we have measured the utilization range of voltage (about 12.5 to 14.5kV_{pkpk}), the voltage frequency (45kHz), the current of the pulses (40 to 300mA) and the pulses charge (20 to 50nC/period).

We could measure the evolution of NO_x concentration versus energy density and we could notice that the presence of water vapor in the mixture increases the NO_x removal from 10% to 30%. In the same time, we could measure an increase of R-NO_x and VOC quantity in by-products. However, the increasing of R-NOx quantity with power is greater than VOC's.

The isotopic labeling of the introduced O_2 with $^{18}O_2$ has improved the understanding of reactional mechanisms and especially oxidation mechanisms with O atoms (due to O_2 and CO_2 fragmentation in the discharge) and with CO (due to CO_2). Then, we could demonstrate the prior role of O_2 in NO oxidation and R-NO_x formation, the role of CO in the formation of the main VOC's (acetaldehyde and propanal) and the exchange of O atoms between O_2 and CO_2.

AKNOWLEDGMENTS

Authors acknowledge ARC GIE-PSA Peugeot-Citroën-RENAULT-ECODEV and Ministère de la Recherche for financial support and M-F. Gonnord for the development of GC-MS analysis.

REFERENCES

[1] R.S. Sigmond, M. Goldman, *Electrical Breakdown and Discharges in Gases* (Part. B), NATO-ASI Series, B89b, Plenum Press (1983)

[2] J.S. Chang, P.A. Lawless, T. Yamamoto, IEEE Transactions on Plasma Science, **Vol. 19, n°6** (1991), 1152-1165

[3] S. Robert, E. Franke, J. Amouroux, "Polluted gases treatment in a corona discharge plasma reactor", Progress in plasma processing of materials (1999)

[4] F. Daou, A. Vincent, S. Robert, E. Francke, S. Cavadias & J. Amouroux, "*Removal of nitric oxide by point to plane and multipoint to plane DBD in exhaust vehicle gases"*, Proceedings of 15th International Symposium on Plasma Chemistry, **Vol. 7** (2001), 3023-3029

[5] H. Suhr, G. Weddigen, "*Reduction of nitric oxide in flue gases by point to plane corona discharge with catalytical coatings on the plane electrode"*, Combust. Sci. and Tech., **Vol. 72** (1990), 101-115

[6] K. Takaki, M.A. Jani, T. Fujiwara, *"Removal of nitric oxide in flue gases by multipoint to plane dielectric barrier discharge"*, IEEE Transactions on Plasma Science, **Vol. 27, n°4** (1999), 1137-1145

[7] K. Takaki, T. Fujiwara, "*Multipoint barrier discharge process for removal of NOx from diesel engine exhaust",* IEEE Transactions on Plasma Science, **Vol. 29, n°3** (2001), 518-523

[8] Y.S. Mok, J.H. Kim, I-S. Nam, S.W. Ham, "*Removal of NO and formation of byproducts in a positive-pulsed corona discharge reactor"*, Ind. Eng. Chem. Res., **Vol. 39** (2000), 3938-3944

[9] A. Vincent, F. Daou, S. Robert, E. Francke, S. Cavadias & J. Amouroux, "*Electrical characterization of DBD wire-cylinder reactor: influence of operating parameters and by-products analysis"*, Proceedings of 15th International Symposium on Plasma Chemistry, **Vol. 7** (2001), 3141-3147

[10] E. Francke, S. Robert, J. Amouroux, "*Hydrodynamic and electrical characterization of a corona discharge plasma reactor"*, High Temperature Material Processes, **Vol. 4, n°1** (2000), 139-150

[11] J-W. Chung, M-H; Cho, B-H. Son, Y-S. Mok, W. Namkung, "*Study on reduction of energy consumption in pulsed corona discharge process for NO_x removal"*, Plasma chemistry and plasma processing, **Vol. 20**, No. 4 (2000), 495-509

[12] D-J. Kim, Y. Choi, K-S. Kim, "E*ffects of process variables on NO_x conversion by pulsed corona discharge process",* Plasma chemistry and plasma processing, **Vol. 21**, No. 4 (2001), 625-650

[13] S.L. Suib, S.L. Brock, M. Marquez, J. Luo, H. Matsumoto, Y. Hayashi, "*Efficient catalytic plasma activation of CO_2, NO, and H_2O"*, J. Phys. Chem. B, **102** (1998), 9661-9666

[14] J. Luo, S.L. Suib, M. Marquez, Y. Hayashi, H. Matsumoto, "*Decomposition of NO_x with low-temperature plasmas at atmospheric pressure: neat and in presence of oxidants, reductants, water and carbon dioxide*, J. Phys. Chem. A, **Vol. 102** (1998), 7954-7963

[15] R. *Dorai, M.J. Kushner*, "*Effect of propene on the remediation of NO_x from engine exhausts",* SAE/SP, n° 1999-01-3683, Toronto (1999)

[16] N.M. Donahue, R. Mohrschladt, T.J. Dransfield, J.G. Andersan, *"Constraining the mechanism of OH +NO_2 Using Isotopically Labeled Reactants: Experimental evidence for HOONO formation",* J. Phys. Chem. B, **Vol. 103** (2001), 10999-11006

[17] R. Gasparik, S. Ihara, C. Yamabe, S. Satoh, "*Effect of CO_2 and water vapors on NO_x removal efficiency under conditions of DC corona discharge in cylindrical discharge reactor"*, Jpn. J. Appl. Phys., **Vol. 39** (2000), 306-309

[18] U. Kirchner, V. Scheer, R. Vogt, "*FTIR spectroscopic investigation of the mechanism and kinetics of the heterogeneous reactions of NO_2 and HNO_3 with soot"*, J. Phys. Chem. A, **Vol. 104** (2000), 8908-8915